



Lawrence Berkeley Laboratory

UNIVERSITY OF CALIFORNIA

Materials & Chemical
Sciences Division

RECEIVED
LAWRENCE
BERKELEY LABORATORY

APR 19 1988

Submitted to Journal of the
Electrochemical Society

LIBRARY AND
DOCUMENTS SECTION

The Corrosion of Carbon Black Anodes in Alkaline Electrolyte: III. The Effect of Graphitization on the Corrosion Resistance of Furnace Blacks

P.N. Ross and M. Sattler

January 1988

TWO-WEEK LOAN COPY
*This is a Library Circulating Copy
which may be borrowed for two weeks.*



LBL-24585
e.2

DISCLAIMER

This document was prepared as an account of work sponsored by the United States Government. While this document is believed to contain correct information, neither the United States Government nor any agency thereof, nor the Regents of the University of California, nor any of their employees, makes any warranty, express or implied, or assumes any legal responsibility for the accuracy, completeness, or usefulness of any information, apparatus, product, or process disclosed, or represents that its use would not infringe privately owned rights. Reference herein to any specific commercial product, process, or service by its trade name, trademark, manufacturer, or otherwise, does not necessarily constitute or imply its endorsement, recommendation, or favoring by the United States Government or any agency thereof, or the Regents of the University of California. The views and opinions of authors expressed herein do not necessarily state or reflect those of the United States Government or any agency thereof or the Regents of the University of California.

THE CORROSION OF CARBON BLACK ANODES IN ALKALINE
ELECTROLYTE: III. THE EFFECT OF GRAPHITIZATION ON THE
CORROSION RESISTANCE OF FURNACE BLACKS

Philip N. Ross and Margaret Sattler

Materials and Chemical Sciences Division
Lawrence Berkeley Laboratory
University of California
Berkeley, CA 94720

This work was supported by the Assistant Secretary for Conservation and Renewable Energy, Office of Energy Storage and Distribution, Electrochemical Energy Storage Division, U.S. Department of Energy under Contract DE-AC03-76SF00098.

THE CORROSION OF CARBON BLACK ANODES IN ALKALINE
ELECTROLYTE: III. THE EFFECT OF GRAPHITIZATION ON THE
CORROSION RESISTANCE OF FURNACE BLACKS

Philip N. Ross and Margaret Sattler
Materials and Chemical Sciences Division
Lawrence Berkeley Laboratory
University of California
Berkeley, CA 94720

ABSTRACT

A selection of furnace black carbons of varying surface area and industry type were heat-treated in purified helium at 2700°C and the corrosion resistance measured under conditions of oxygen evolution in 30% KOH at 55°C. The extent of graphitization was determined qualitatively by x-ray diffraction and by transmission electron microscopy (TEM). Separate linear correlations of the corrosion rate per unit mass with the BET surface area were observed for furnace blacks and for graphitized furnace blacks, with the rate for the graphitized blacks being a factor of ca. 2.5 lower on a unit area basis. The correlations had a relatively high standard deviation, however, indicating that BET area was probably not the only physical property affecting the corrosion rate. TEM analysis of the carbons after extended corrosion indicated a strong preferential attack of the ungraphitized regions, i.e. much greater selectivity than the factor of 2.5 indicated by the BET correlation. A unifying correlation was observed for both the furnace blacks and their graphitized forms using the corrosion rate per unit mass and the iodine adsorption number. It was concluded that there are specific sites on the carbon surface (titrated by iodide) that serve as the initiators for dissolution of

carbon atoms from the bulk of the material. One particular type of furnace black, SRF (N774), appears to be an especially good precursor for forming a highly graphitized and very corrosion resistant carbon black.

Introduction

In previous studies [1,2], we reported the determination of the product distribution from the corrosion of acetylene black under conditions of oxygen evolution in alkaline electrolyte, and the effect of evolution catalysts on both the product distribution and the overall rate of loss of carbon. We also showed by transmission electron microscopy (TEM) that acetylene black is not a microstructurally homogeneous material, and that one might expect there to be preferential attack of some microstructures in acetylene black. However, we were unable to find definitive evidence of preferential attack.

In the present work, we provide definitive evidence of preferential corrosion of the amorphous microstructural regions of acetylene black, and high resistance to corrosion of graphitic microstructural regions. This observation is extended to a selection of furnace black carbons of varying surface area and industry type which were graphitized by heat-treatment in an inert atmosphere at 2700°C. The extent of graphitization was determined qualitatively by x-ray diffraction and by high resolution TEM, and the effect of graphitization on the corrosion resistance of the carbon black was determined using the methods reported previously [1,2]. A possibly more quantitative measure of graphitization is suggested by the correlation found here between corrosion rate and iodide adsorption, provided that iodide is adsorbed only on the edge-plane of graphite. Validation of the latter will require further study of the structure specificity of iodide adsorption. It is clearly shown, nonetheless, that graphitization has an effect on the corrosion resistance that is much more dramatic for

some types of furnace blacks than for others, the difference clearly being the completeness in the conversion of the microstructure to the graphitic form.

Experimental

Table I lists the furnace process carbon blacks used in this study with the (rubber) Industry Classification and the ASTM (D-1765) Classification where applicable [3]. All the carbon blacks were obtained either from Ashland Chemical (Columbus, OH) or from Cabot (Billerica, MA), with the exception of acetylene black, which we obtained from Shawinigan. BET surface areas were measured using standard methods and apparatus (Quantasorb). The furnace process carbon blacks were heat-treated in a graphite element furnace (Astro Industries, Santa Barbara CA) in pre-purified helium. The samples were placed in graphite boats, and heated to 2700°C at a rate of ca. 100°C per minute, held at that temperature for 2 hrs., then cooled at approximately the same rate to room temperature. Iodide adsorption measurements were done according to the rubber industry standard procedure designated as ASTM D-1510 [10]. The experimental procedure for the corrosion measurements was the same as that described previously [1,2]. The observed total anodic current was corrected for the rate of oxygen evolution (measured independently with a mass spectrometer) to obtain the corrosion current. The corrosion current was converted to weight loss using Faraday's law for $n=4$, since our product distribution analysis showed that carbonate formation was the predominant corrosion

process at the conditions used, e.g. 30% KOH, 55°C, 350-550 mV vs. Hg/HgO. All potentials refer to an external Hg/HgO reference electrode in the same electrolyte.

Results

Time dependence of the current:

As we mentioned in our previous reports on the anodic processes occurring with acetylene black, the time dependence of the current-potential relationship for carbon blacks in the potential region of 400-600 mV in KOH is quite complex, and deserves further discussion in the context of this work. The short time response of the total anodic current is shown in Figure 1 for graphitized RCF carbon, with the potential set initially at 320 mV and progressively increased after the time shown in the figure. There are two time domains to the current, one on the scale of minutes, where the current drops exponentially in time, and a second domain on the scale of hours where the current assumes a quasi-steady value. The exponential region was characterized by an absence of any detectable amount of corrosion product external to the electrode (either in solution or in gas phase), indicating the charge passed in this time corresponds to surface processes, i.e. the oxidation products remained on the carbon surface. The potential dependence of these surface processes was complex, and displayed charge-accumulation behavior. For example, the largest amount of charge accumulated in the exponential time regime was passed at the first potential set, after immersion of the electrode, and

increasing the potential added a progressively decreasing amount of charge, until at 520 mV and above the exponential region disappeared, i.e. no further charge was added to the charge accumulated at lower potentials. Thus, the anodic processes occurring in the exponential time regime have some similarities to the anodic surface processes that occur on noble metals like Pt and Au, i.e. anodic polarization produces a significant transient anodic current without producing any measurable quantity of reaction product external to the electrode (charge accumulates on the surface of the electrode as surface oxide). However, these processes are not the corrosion processes that were the subject of our previous studies of the corrosion of acetylene black [1,2], and they are not the subject of our study here. As before, we define the corrosion processes of interest here as the processes producing corrosion products external to the electrode surface, i.e. processes causing a true loss of carbon from the electrode with time. Our analysis, therefore, concentrated on the quasi-steady state time regime (on the scale of 1-10 hrs.) in which a reasonable material balance was obtained, and all of the charge could be attributed either to carbon dissolution or to oxygen evolution. For the purposes of comparison of the carbons to one another, we chose a standard potentiostatic test, consisting of a "break-in" period of 15 hrs. at 450 mV, followed by 5 hrs. at 550 mV. The current after the latter period, corrected for the partial current for oxygen, was used as the measure of the corrosion resistance of the carbon.

Carbon microstructure:

As we described in our previous study [1], acetylene black has a heterogeneous microstructure, as clearly indicated by high resolution TEM analysis. There are regions in the acetylene black where graphitic ribbons are apparent, as seen in the region shown in Figure 2. The regions around these ribbons have either a turbostratic [3] structure or are truly amorphous. One might expect that these regions would exhibit different corrosion resistance, and we were able to find definitive evidence that this is the case. Figure 3 shows the same carbon after corrosion in the cell at 550 mV at 55°C for 20 days, with a weight loss exceeding 50%. The region of the post-test material shown at high magnification in Figure 3a indicates that essentially the only carbon microstructures remaining were the graphitic ribbons. This is even more graphically illustrated by the low magnification micrograph of another region shown in Figure 3b.

In contrast, the furnace blacks all have very homogeneous microstructures of the turbostratic type [3]. There are systematic variations in the structure on a larger scale that may have an important effect on the graphitization process. This variation is in the prime particle size and the way in which the prime particles are fused together to form agglomerates. Figure 4 compares the agglomerate structure of HAF to SRF carbon, the former having about three times the BET area of the latter. Note the much larger prime particle size, and the more highly fused structure of the prime particles in the SRF carbon, with the complete absence of microporosity in the agglomerate

structure. It is the microporosity that creates the much higher BET area of the HAF carbon. Figures 5 and 6 show the micrographs of graphitized SRF carbon, with the striking conversion of the smooth spherical shapes to irregular angular shapes formed from graphite bands winding around each other. The BET area actually increased following graphitization of SRF carbon, the only carbon in which this occurred. The graphite layer planes are remarkably flat in some regions of the structure, and contain as many as 70 layer planes in some bands (Figure 6). The other graphitized blacks had a much more heterogeneous microstructure. Figure 7 shows a micrograph of graphitized HAF carbon, which also has formed graphitic bands, but they are not as well-ordered (note the waviness in the planes) nor are they composed of as many layer planes. Also, there were large regions of residual amorphous or turbostratic carbon remaining, typically about one-half of the material was still in this form. The size of the prime particles of the furnace blacks and the thickness of the graphitic bands (L_c) in the graphitized furnace blacks are reported in Table I.

X-ray diffraction analyses of the carbon structures produced a qualitatively similar picture of the microstructure. Figure 8 shows the XRD pattern for SRF and graphitized SRF. The peaks have been indexed following the notation of Warren [8], and the interpretation of the changes in the pattern made here follows Warren as well. The pattern for SRF carbon black is characteristic of the turbostratic structure, with very poor alignment of the layer planes to one another,

e.g. absence of the high order (004) and (006) crystalline reflections. The 2700°C heat treatment produced aligned layer planes, but the asymmetry of the (100) and (110) crystalline peaks indicates rotational misalignment of the planes, i.e. ABC stacking rather than ABA stacking. The sharpness of the (002) peak indicates large repeat distances for the layer plane stacking, e.g. ca. 20 nm, in reasonable agreement with what was observed by TEM. The patterns for the other heat-treated furnace blacks were qualitatively similar to that for heat-treated SRF, but important differences could be distinguished. The pattern in Figure 9 is for heat-treated HAF (N330). Two distinctions from heat-treated SRF can be made: the (001) reflections are not as sharp nor as well resolved; there is a broad peak at ca. $17^\circ 2\theta$ that is not present in other carbon. The first distinction is comparable to the one made in Figures 5-7 with TEM, namely that the layer planes are not as well aligned nor are the number of stacked planes as large in the HAF as in the SRF carbons following identical heat-treatments. The broad peak at 17° appears to correspond to the amorphous regions of the HAF carbon observed even after heat-treatment. A broad peak at 17° was reported by Jenkins et al. [9] for pyrolyzed resins which they characterized as non-graphitizing, i.e. they form polymeric or "glassy" carbons as opposed to a graphite.

Corrosion rates:

The corrosion rates for the various carbons are tabulated in Table I and plotted versus BET area in Figure 10. There appears to be a separate linear correlation for the furnace black carbons and for the

graphitized carbons, the former having a slope, i.e. corrosion rate per unit area, a factor of 2.5 higher. However, the standard deviation of the individual points about each of the best-fit lines is quite large, 14%. This is much higher than the precision with which either the BET area or the corrosion rate could be measured. Further, the deviations are not random, but for both sets they appear to be "s-shaped", suggesting that there is a fundamental property other than area that must be accounted for even within each separate class of carbon. Figure 11 shows the plot of corrosion rate versus the iodine adsorption number, which is the quantity of iodide adsorbed per unit mass of carbon. In this case, both ungraphitized and graphitized carbons are fit with a linear correlation with a standard deviation of 4%, a significant improvement over the fit with BET area.

Discussion

The material balance obtained for the corrosion process in the quasi-steady state time domain indicated that the primary anodic reaction in this time frame is the dissolution of carbon to form carbonate in solution [1]. This weight loss process followed a transient period in which the principal process was surface oxidation, apparently to a critical level of surface charge. Unfortunately, the poor reproducibility of the data for this process in these experiments did not enable us to establish the quantity of this critical charge to better than an order of magnitude, ca. $10^2 \mu\text{C}/\text{cm}^2$ (BET). The transient period requires much further and more detailed study, and should employ

smaller (thinner) electrodes in a more controlled geometry, e.g. a microelectrode. The surface oxides formed are not passive, in the sense that anodic layers on metals are often passive, since the rate of oxidation dropped by only a factor of 2-3 instead of one or more orders of magnitude. It is not, however, known whether the oxide groups actually dissolve, or merely form and remain while other surface carbon atoms are selectively dissolved directly into solution. This important level of mechanistic detail will be the subject of future studies in our laboratory.

If the corrosion rate per unit mass of a material is not directly proportional to its surface area, then it is likely that some regions of the material are attacked preferentially to others. As we found here, the corrosion rate of either the graphitized carbons or their furnace black precursors was not well correlated by surface area, and electron microscopy showed that the amorphous microstructural carbon was attacked preferentially to highly graphitized microstructural regions. While microscopy was a very effective tool for analyzing the microstructural diversity, it was not an effective tool for quantitative analysis of how much of what type of microstructure was present. X-ray diffraction analysis is also difficult to use quantitatively, since the x-ray scattering power of a solid depends on its structure, e.g. an amorphous structure for a given element produces a lower scattered intensity than a crystalline structure of the same element. If the carbon microstructures exhibited other kinds of chemical selectivity, then that selectivity could be used as a more quantitative

measure of the amount of different structures present. Chemisorption methods could be useful in identifying at least the surface sites that serve as the nuclei for the initiation of corrosion (dissolution) reactions. To apply the chemisorption method to our purpose here, we looked for a correlation between the amount of a specific species adsorbed and the corrosion rate. As shown by Figure 11, a unifying correlation for both the graphitized and ungraphitized forms was observed between the corrosion rate per unit mass and the amount of iodide adsorbed per unit mass. From this result alone, it appears that there are specific sites on the carbon surface, titrated by iodide, that serve as the initiators for the dissolution of carbon atoms from the surface.

The chemistry of sites adsorbing iodide (in the ASTM method) is not well-known. The ratio of the iodine number to the BET area is a measure of the number of sites adsorbing iodine per unit area of surface. Inspection of Table I shows that this ratio has its maximum value for the furnace black carbons, is approximately the same for all the carbons prior to heat treatment, and that after graphitization the ratio is 3-5 times lower. The ratio is the smallest for the carbon with the highest degree of graphitization (as measured by the thickness of the layer planes). These correlations indicate that iodine is probably not adsorbed on the basal plane of graphite, and is selectively adsorbed on either/both the amorphous ungraphitized regions or/and the edge-planes of the graphitized regions, since in all cases the graphitized carbons had some regions of amorphous material that

remained ungraphitized. For the furnace black carbons, which have no basal plane area, it appears likely that iodine adsorbs on the entire physical surface, just as nitrogen does in the BET method. But in the graphitized blacks, where the ratio was 3-5 times lower, iodine adsorption appeared to occur on only 20-30% of the physical surface, probably due to the presence of basal plane area not adsorbing iodine. The TEM results for the graphitized carbons indicated that a basal plane area as high as 70-80% of the total surface area is not unreasonable.

There is no mention of iodide adsorption as a specific titrant for edge-plane sites on graphitic materials in the carbon chemistry literature. Carbon chemists use the preferential adsorption of n-paraffins from mixtures of branched paraffins to measure the basal-plane sites, and the adsorption of alcohols to measure edge-plane sites [4]. We have not used these hydrocarbon adsorption methods on our materials to date, as the methodology is considerably more complex than the iodide method. The work by Yeager and co-workers [5-7] suggests the use of capacitance measurements to measure the edge-plane area, since the capacitance of the basal-plane is an order of magnitude smaller than that of the edge-plane. In our experience, we did not find capacitance measurements of these carbons to be sufficiently reproducible, with the capacitance being very sensitive to the electrochemical pretreatment of the carbon and the method of forming the carbon into an electrode.

It is clear that graphitization has a beneficial effect on the corrosion resistance of furnace black carbons, and that the effect is

fractionally much greater for some types of carbons. In particular, graphitization of SRF type carbon lowered the corrosion rate per unit mass by a factor of 7, while in most carbons the effect was only a factor of 2-3. This material was also the most completely graphitized carbon, as judged from both x-ray diffraction and electron microscopy. The other graphitized furnace blacks had a considerable amount of carbon remaining in the original turbostratic or amorphous form, and the graphitic regions were not as close to the true graphite structure, e.g. wavy layer planes. From a technological standpoint, graphitized SRF type carbons appear to be the most promising class of carbons for applications utilizing carbon materials in oxygen evolving anodes.

Acknowledgements

The authors are indebted to Dr. Marvin Deviney (Ashland Chemical) and Mr. Larry Newman (Cabot) for contributing carbon materials for these studies. This work was supported by the Assistant Secretary for Conservation and Renewable Energy, Office of Energy Storage and Distribution, Electrochemical Energy Storage Division, U.S. Department of Energy under contract DE-AC03-76SF00098. The electron microscopy in this work was done at the National Center for Electron Microscopy at the Lawrence Berkeley Laboratory. Operating funds for the Center are provided by the Assistant Secretary for Energy Research, Office of Basic Energy Sciences, Materials Sciences Division, U.S. Department of Energy, under contract DE-AC03-76SF00098.

References

1. P. N. Ross and H. Sokol, J. Electrochem. Soc. 131(1984)1742.
2. N. Staud and P. N. Ross, J. Electrochem. Soc. 133(1986)1079.
3. Kirk-Othmer Encyclopedia of Chemical Technology, Volume 4, John Wiley and Sons, New York, 1978, Third Edition, pp. 631-66.
4. A. J. Groszek and G. I. Andrews, "Some Adsorptive Properties of Polar and Basal Plane Sites in Graphite", Society of the Chemical Industry (UK), London, 1971, pp. 156-64.
5. J. P. Randin and E. Yeager, J. Electrochem. Soc. 118(1971)711.
6. _____, J. Electroanal. Chem. 36(1972)257.
7. _____, J. Electroanal. Chem. 58(1975)313.
8. B.E. Warren, "X-Ray Study of the Graphitization of Carbon Black", Proceedings of the First and Second Conferences on Carbon, Waverly Press, Baltimore MD, 1956, pp. 49-58.
9. G. M. Jenkins, K. Kawamura and L. L. Ban, Proc. Roy. Soc. Lond. A, 327(1972)501.
10. "Standard Method of Testing Carbon Black - Iodine Adsorption Number," Annual Book of ASTM Standards, Part No. 37, 1982, pg. 379.

Table I. Correlation of Physical Properties of Carbon Blacks and Corrosion Resistance

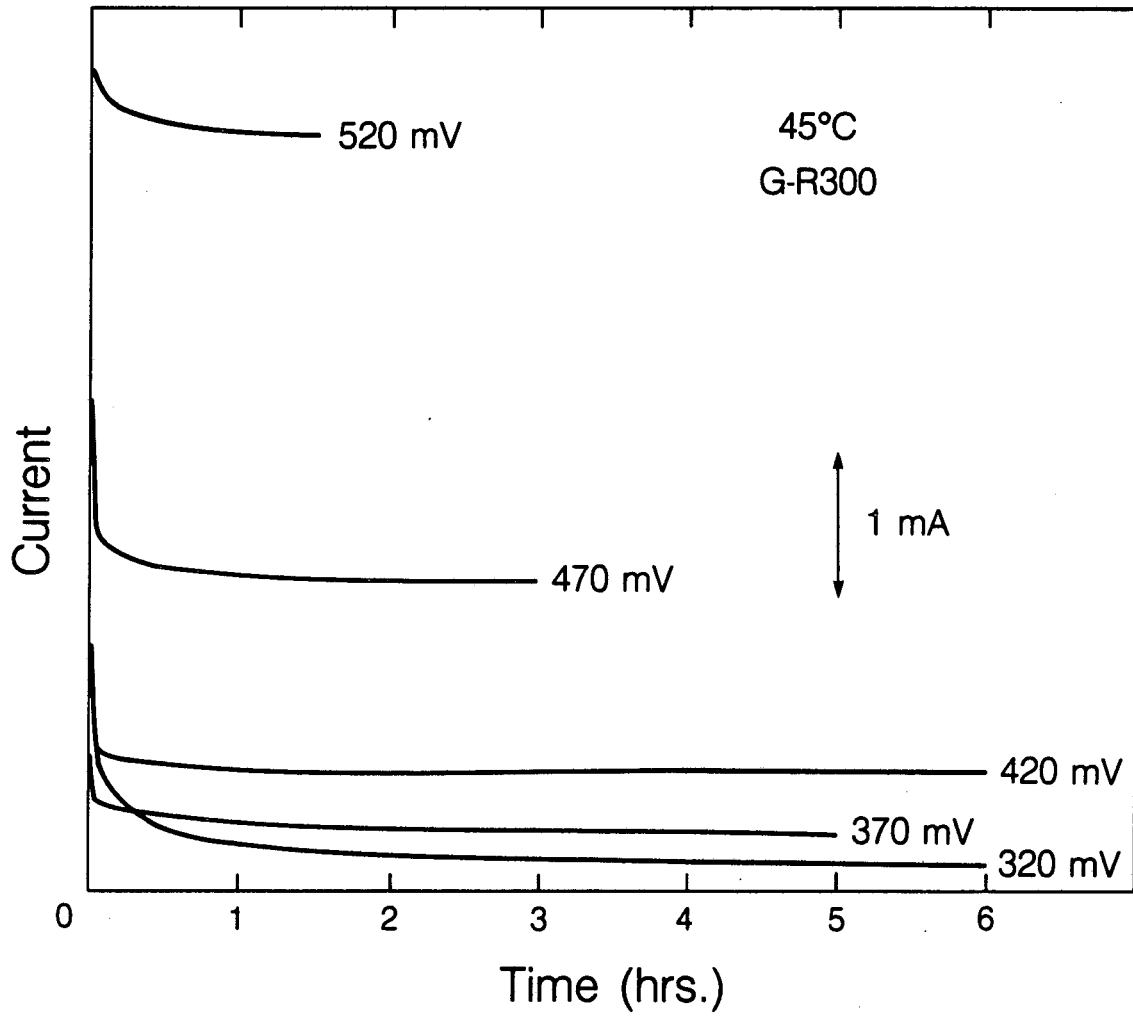
Carbon Type	BET Area (m ² /g)	Iodine Adsorption (mg/g)	IAN/BET Ratio (mg/mg ²)	Particle ¹ Size (nm)	Corrosion ² Rate (% hr ⁻¹)
HCF-1	560	-	-	13	>10
HCF-1 Graphitized	220	105	0.48	-	0.5
XCF	254	270	1.06	30	2.0
XCF Graphitized	128	65	0.51	3(L _c)	0.6
SAF (N110)	115	145	1.26	-	1.5
SAF Graphitized	85	55	0.65	-	0.5
HAF (N330)	80	82	1.03	27	1.0
HAF Graphitized	70	32	0.46	3(L _c)	0.3
RCF	85	83	0.98	25	0.5
RCF Graphitized	70	35	0.50	3(L _c)	0.15
SRF (N774)	25	32	1.28	80	0.15
SRF Graphitized	32	7	0.25	30(L _c)	0.02
Acetylene black	70	35	0.50	30	0.10

¹Size of prime particles determined by electron microscopy. L_c denotes measurement of thickness of graphite layers.

²In 35% KOH at 50°C at 550 mV (Hg/HgO). See text for complete description of corrosion measurement.

Figure Captions

- Figure 1. Potentiostatic current-time curves for an RCF-type carbon black electrode held at successively increasing potentials. 35% KOH at 45°C.
- Figure 2. TEM of acetylene black as-received.
- Figure 3. TEM of acetylene black after extensive corrosion during oxygen evolution at 550 mV at 55°C: a.) at high magnification; b.) a different region at low magnification.
- Figure 4. High resolution TEM of a.) an HAF type carbon black and b.) an SRF type carbon black. Images are at comparable magnification. "P" designates prime particles, "A" designates aggregates of prime particles.
- Figure 5. High resolution TEM of graphitized SRF carbon showing the conversion of the smooth spherical prime particles to graphite banded structure.
- Figure 6. Very high resolution TEM of graphitized SRF showing the a region of 71 graphite layer planes with a high degree of parallelism.
- Figure 7. Very high resolution TEM of graphitized HAF carbon showing a region with 50 layer planes with a high dislocation density.
- Figure 8. X-ray diffraction patterns comparing SRF carbon a.) before and b.) after graphitization. Cu K_{α} .
- Figure 9. X-ray diffraction pattern for graphitized HAF carbon.
- Figure 10. Correlation of the steady-state corrosion rate of (o) as-received and (o) graphitized carbon blacks versus BET area. 550 mV, 35% KOH at 55°C. SD = standard deviation.
- Figure 11. Correlation of the steady-state corrosion rate of (o) as-received and (o) graphitized carbon blacks versus iodine adsorption.



XBL 846-8461

Figure 1



Fig. 2

XBB 875-4062



Fig. 3a

XBB 874-3152

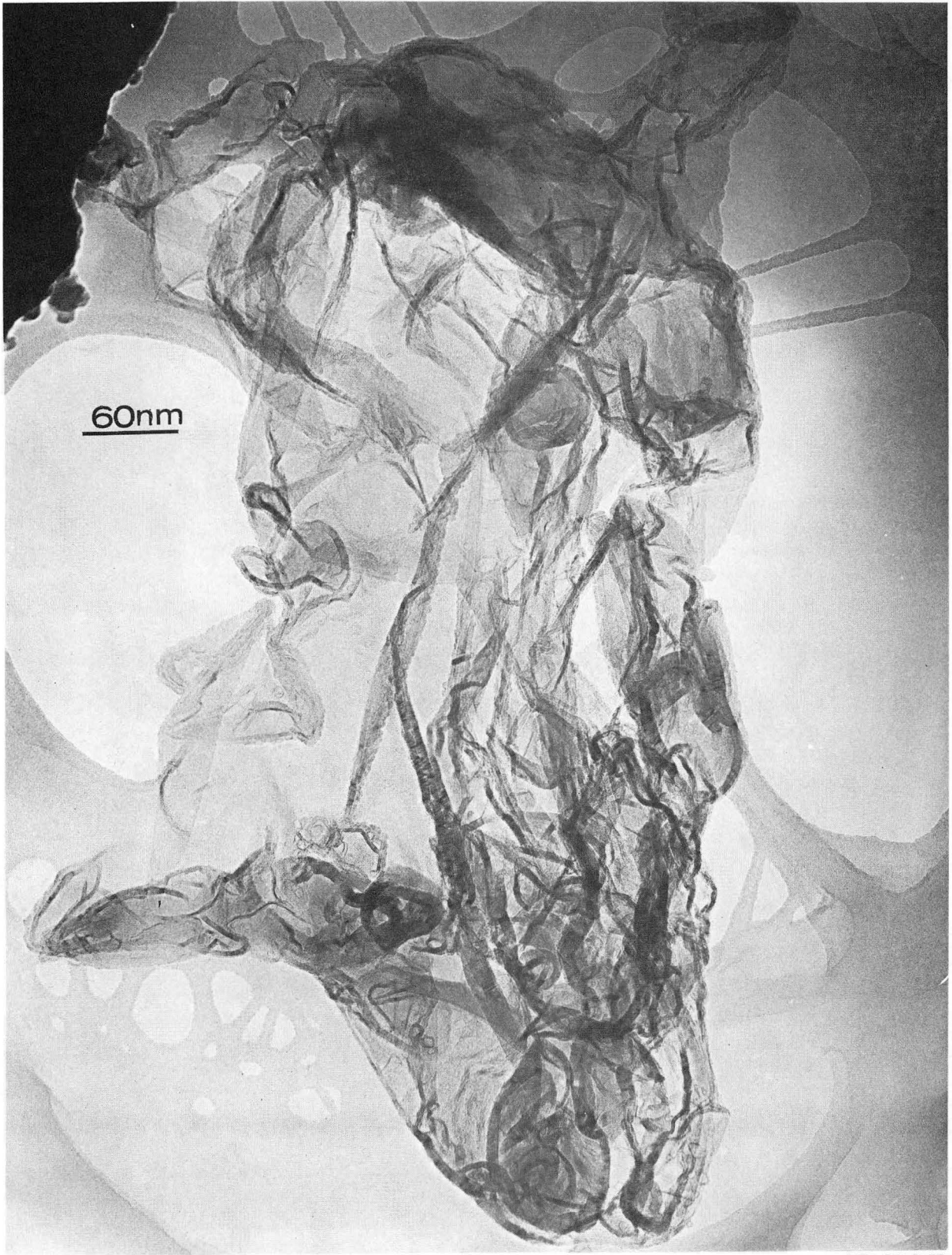


Fig. 3b

XBB 874-3153a

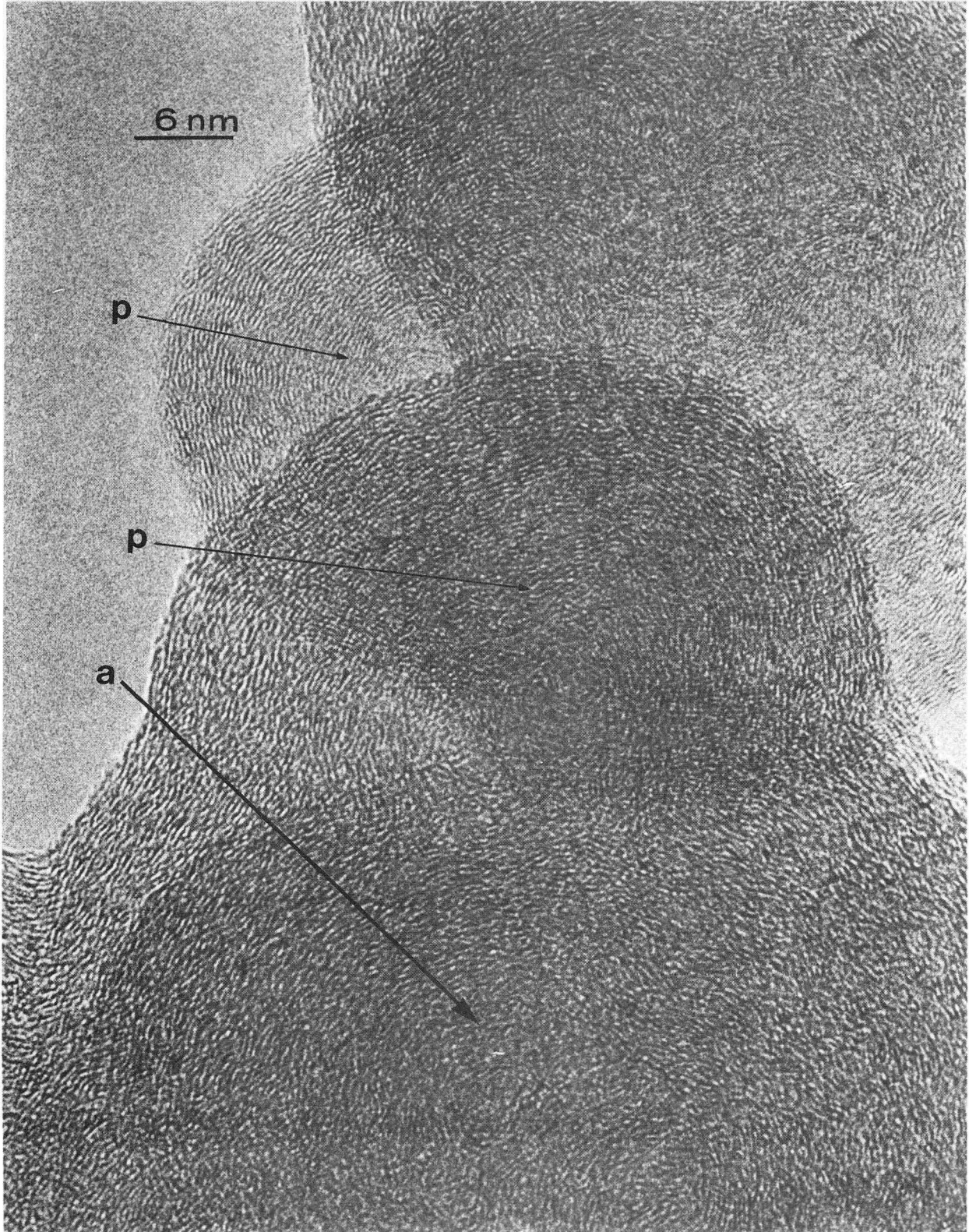
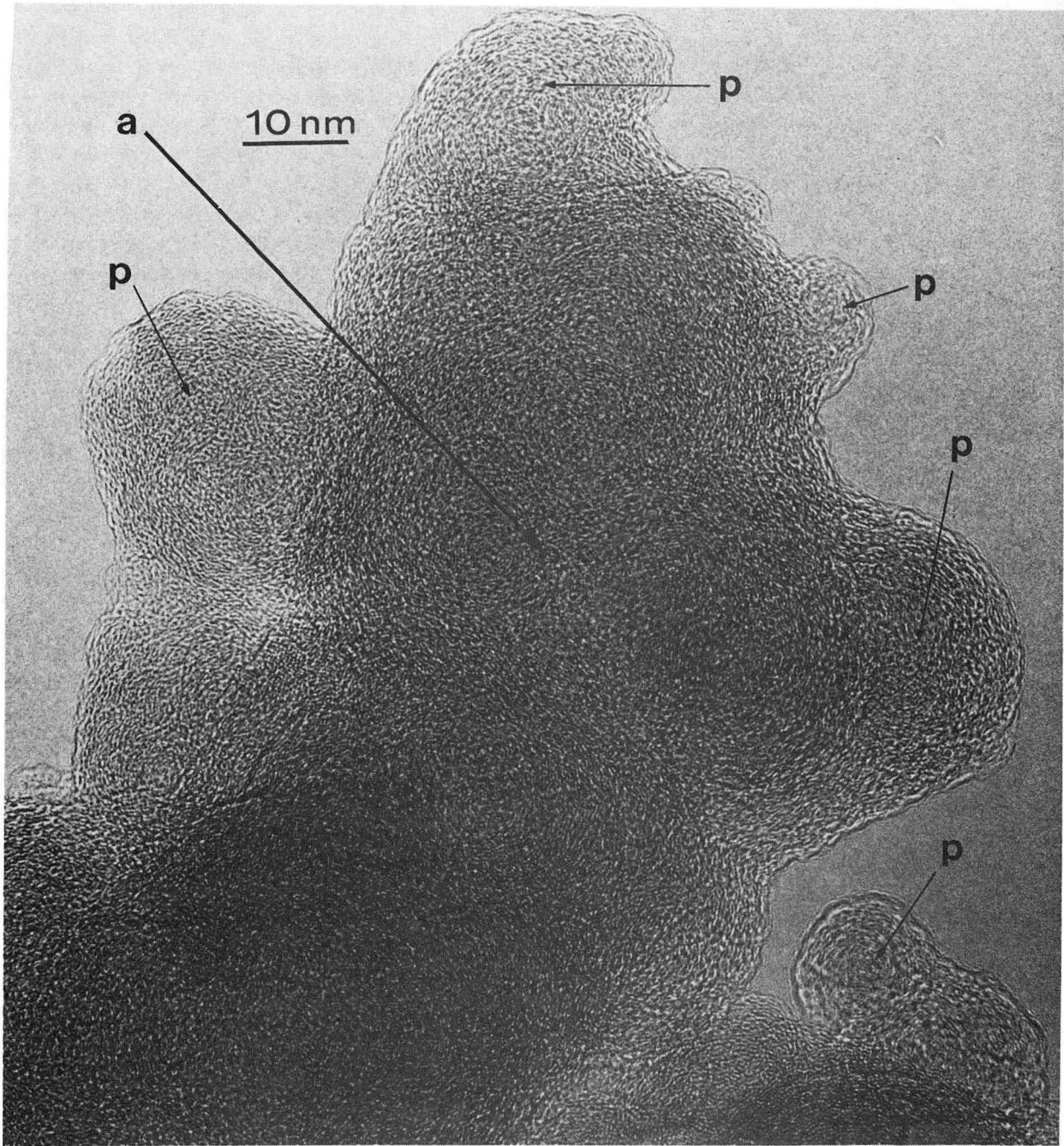


Fig. 4a

XBB 874-3149a



XBB 875-4063a

Fig. 4b



Fig. 5

XBB 874-3151

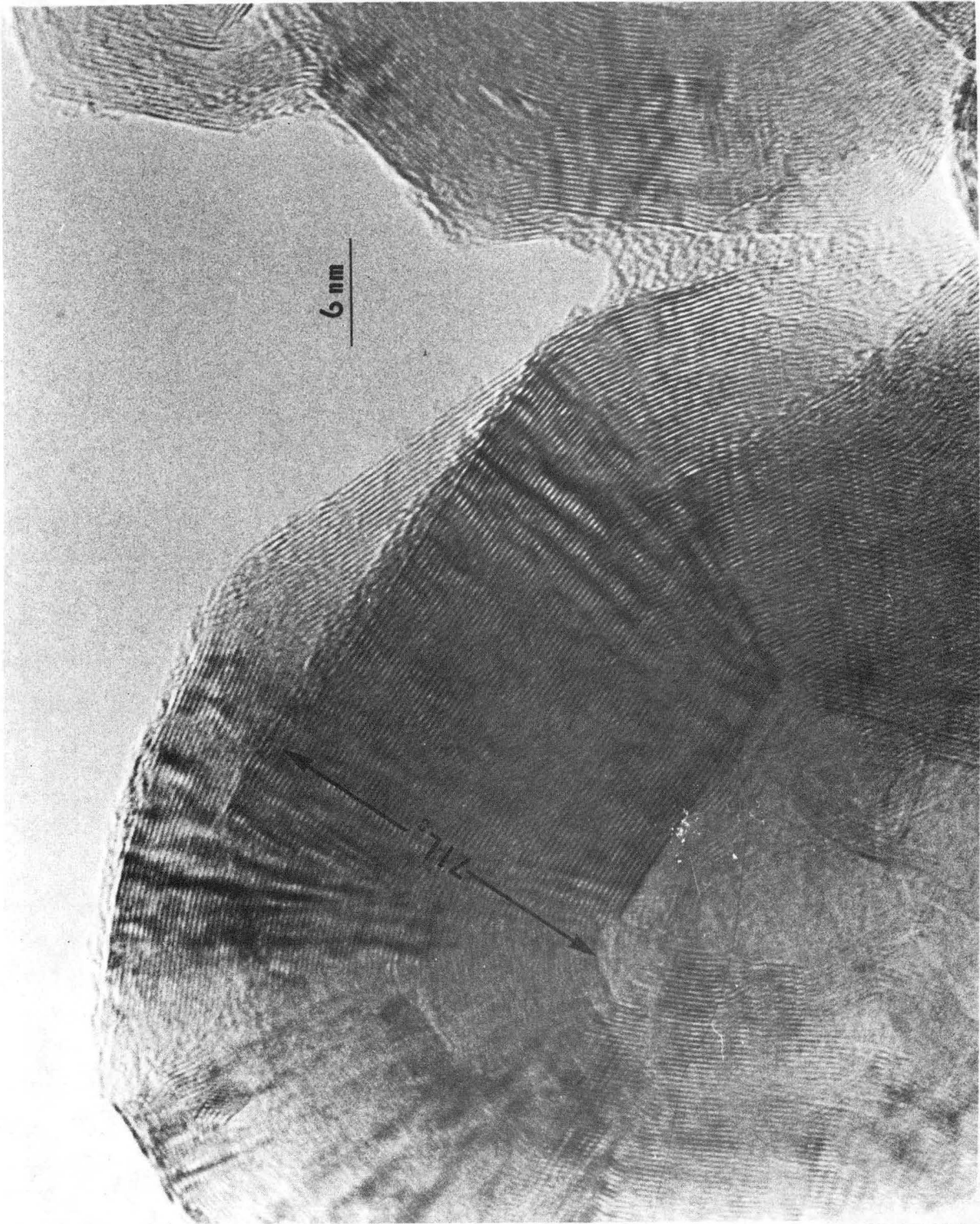


Fig. 6

XBB 850-9218

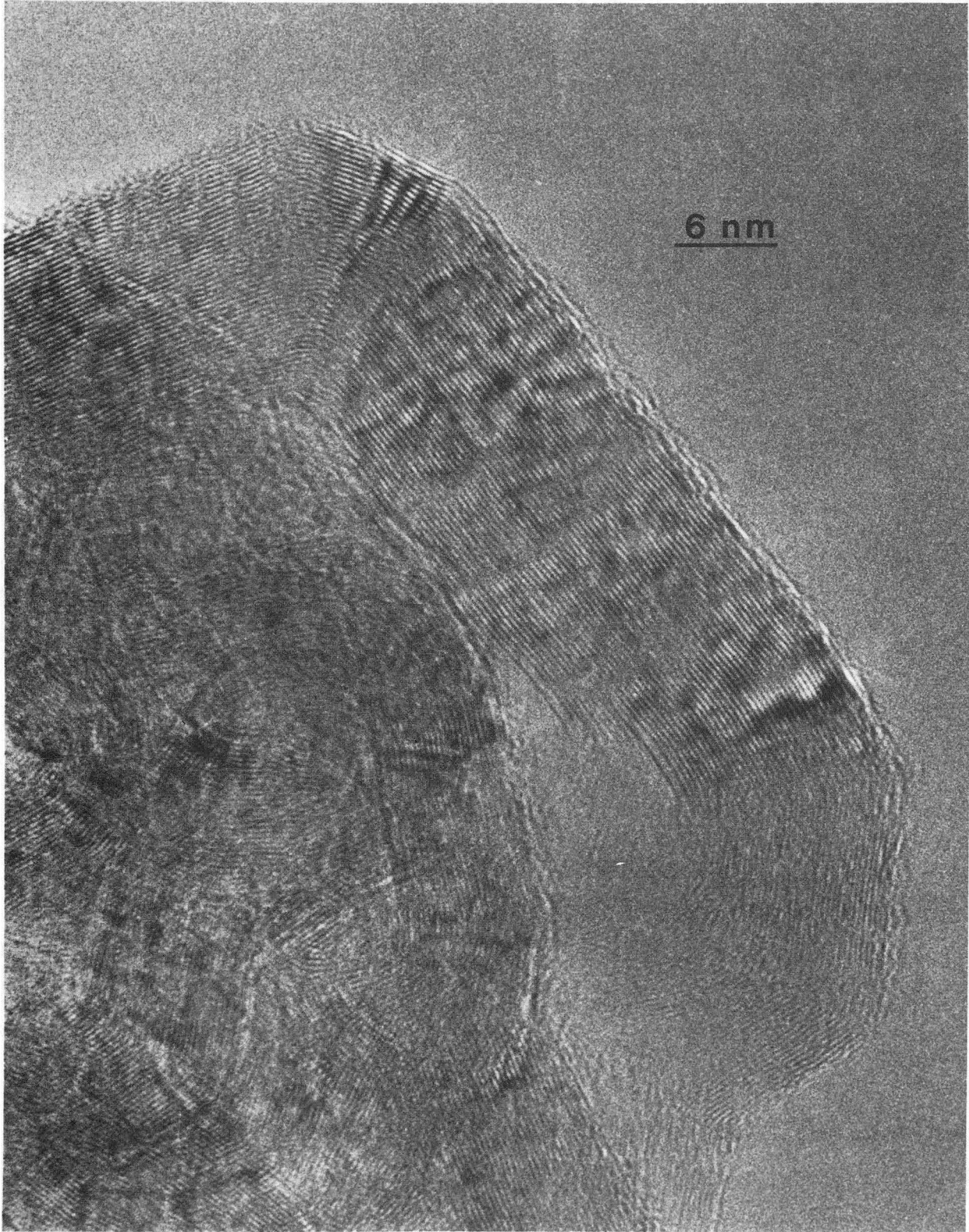
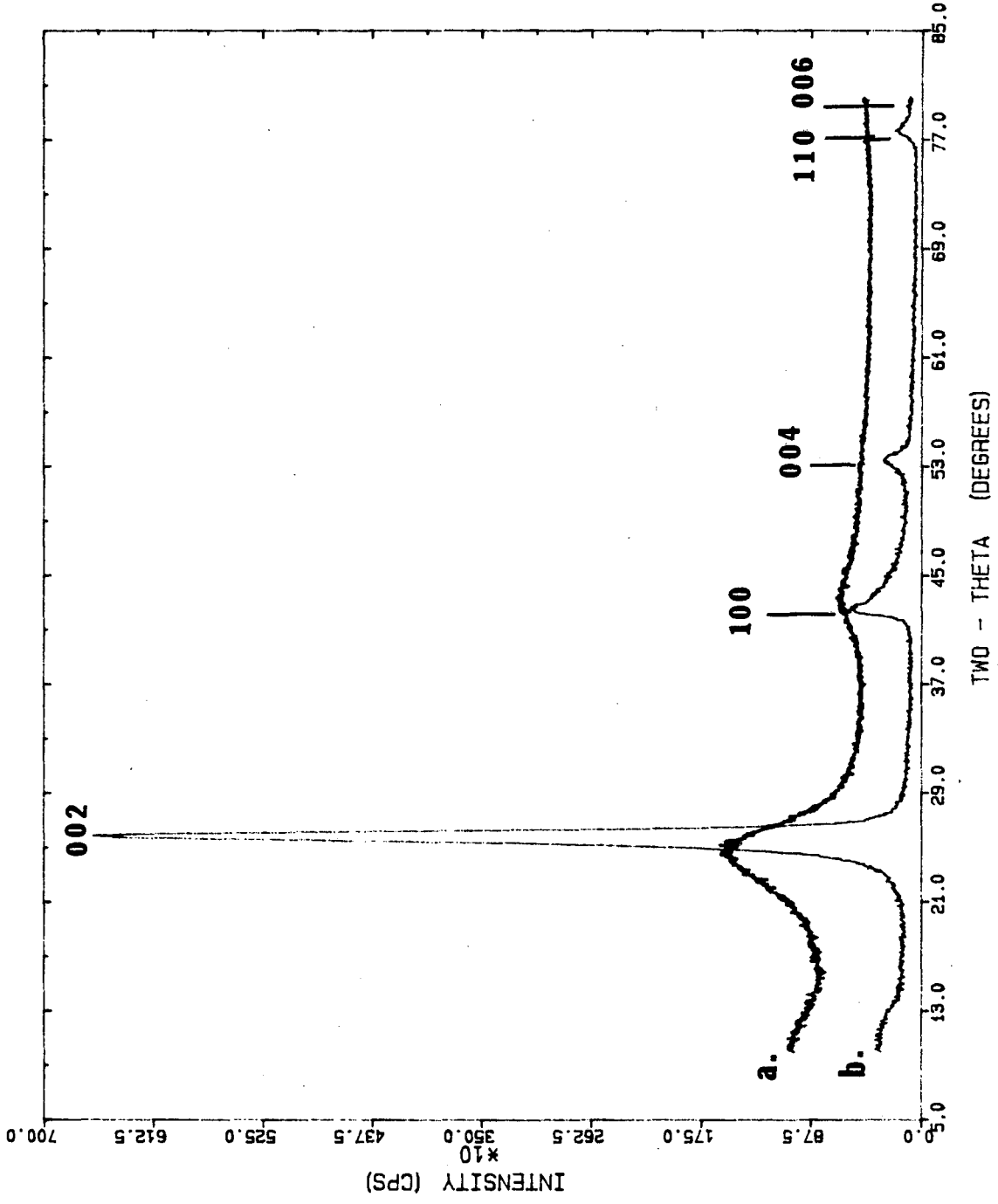


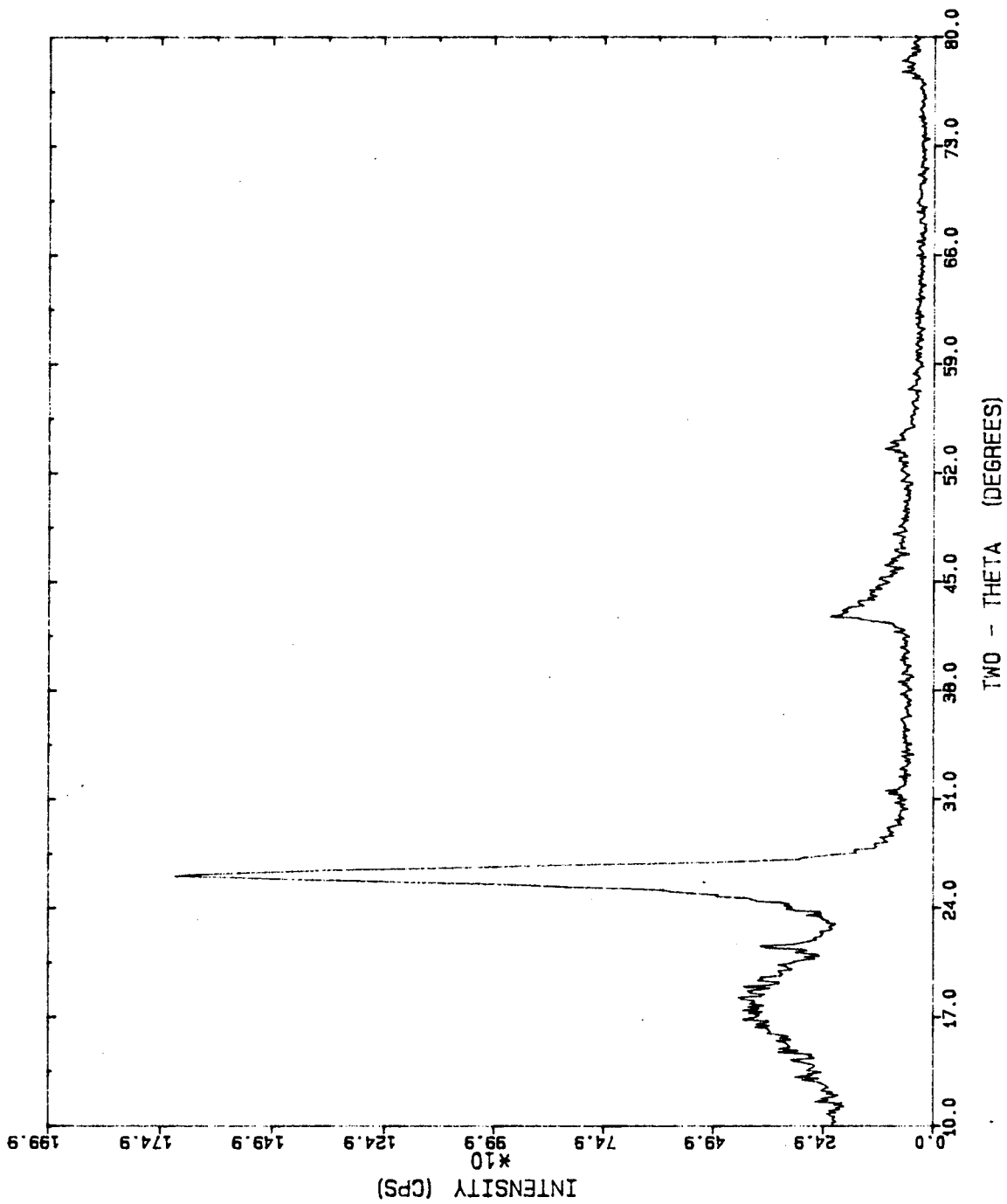
Fig. 7

XBB 874-3150a



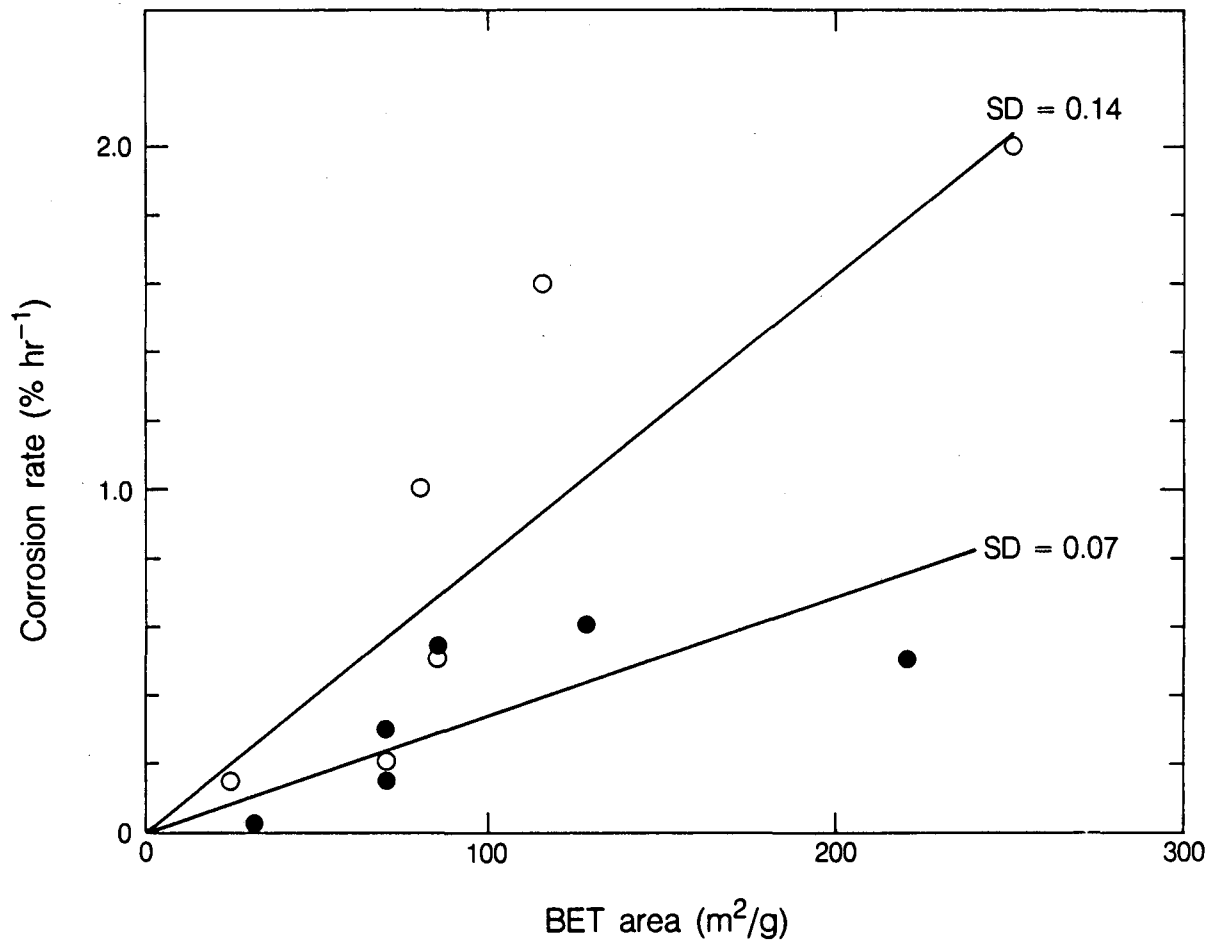
XBL 874-1790

Figure 8



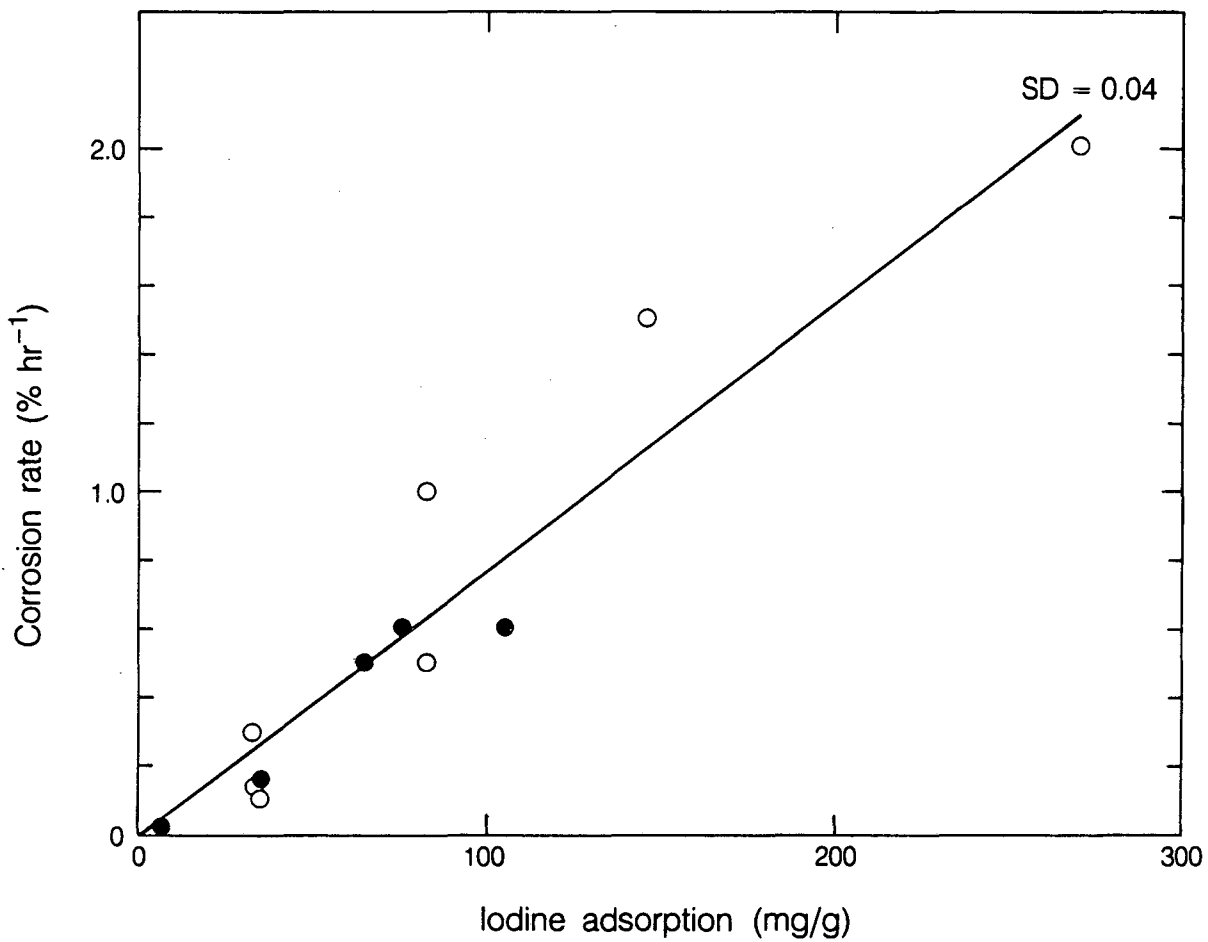
XBL 874-1791

Figure 9



XBL 8511-12509

Figure 10



XBL 8511-12510

Figure 11

*LAWRENCE BERKELEY LABORATORY
TECHNICAL INFORMATION DEPARTMENT
UNIVERSITY OF CALIFORNIA
BERKELEY, CALIFORNIA 94720*